OPTICAL RESPONSE AND SURFACE PHYSICAL PROPERTIES OF THE LUNAR REGOLITH AT REINER GAMMA FORMATION FROM CLEMENTINE ORBITAL PHOTOMETRY: DERIVATION OF THE HAPKE PARAMETERS AT LOCAL SCALE. P. C. Pinet, A. Cord, S. Chevrel, Y. Daydou, UMR 5562/ CNRS/ Toulouse III University, Midi-Pyrenees Observatory, 14 Av. E. Belin, 31400 Toulouse, France.

Introduction: In the last decade, integrated telescopic and spaceborne photometric observation of planetary regolith has progressively evolved from whole-disk toward disk-resolved measurements at regional scales [e.g.,1,2,3,4,5], and more recently toward local scale studies [e.g.,6,7,8,9].

Intriguing areas named swirls have been identified for long as they display regional and local anomalous photometric behaviors. In particular, previous investigations conducted from UVVIS telescopic and Clementine spectral images have established the peculiar optical behavior of the lunar regolith at Reiner Gamma Formation [6,9,10,11]. We present here the derivation of the set of Hapke parameters for this area, using a multiangular dataset derived from Clementine orbital imaging.

Data processing and analysis: We have selected images produced by Clementine along the orbits 322, 58, 190, acquired at wavelength 900 nm (« luc » images),with no or minimal compression rate so that the image radiometric content is not degraded. Instrumental calibration, resampling, coregistration, stacking and binning procedures taking into account the SNR and spatial resolution performances have been applied and a controlled dataset comprising 12 geometric configurations ranging between 7 and 60 ° phase angle values has been generated for a common field of view (referred to in the following as ROI (Region Of Interest)) covering part of the Reiner Gamma Formation and its immediate vicinity with a spatial resolution of 900m/pixel (see Fig.1).

The semi-empirical model developed by Hapke is widely used to analyze reflectance data from planetary surfaces. It requires the knowledge of six parameters to calculate the bidirectional reflectance. Its application relies on some physical quantities characterizing the optical properties of the materials under examination: the phase function, the opposition effect, and the roughness.This study presents a method, based on a genetic algorithm, for the determination of the global set of parameters involved in Hapke's model for planetary surfaces when considering a set of angular conditions representative of the usual range from spaceborne observation in planetary exploration [12]. The principal advantages in applying this technique are: - i) all Hapke's parameters are treated simultaneously with no a priori additional assumptions, thus limiting the risk of meeting a local extreme ; - ii) as an improvement to Monte Carlo method [13], the genetic algorithm optimizes calculation time.

In the present case, we use a "direct encoding" method where a chromosome corresponds to a sequence of Hapke's parameters: it consists in a string composed of six genes: (b, c , h, B0, $\bar{\theta}$, *w),* where b and c correspond to the parameters of the Henyey- Greenstein phase function, h and B0 are the angular width and amplitude of the SHOE opposition function, $\bar{\theta}$ is the macroscopic roughness parameter, and *w*, the single scattering albedo at a given wavelength. Thus, a chromosome contains all the information required to model the bidirectional reflectance as a function of incidence and emergence angles. Since we deal with a large number of potential solutions, we determine the best chromosome allowing the model to fit measured reflectance, and the standard deviation set on each parameter estimate.

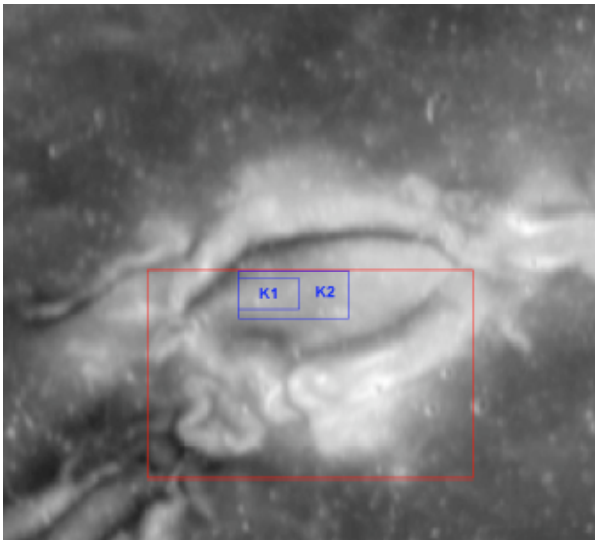

Figure 1. ROI, contoured in red, is the region where the derivation of Hapke parameters has been made for each pixel. K1 and K2 correspond to areas studied by [6].

Results and Interpretation

Given the limited set of configurations (only 3) available with a phase angle g less than 20° (g=7.5, 8.1 and 8.5°), the opposition function (SHOE type) parameters B0 (amplitude) and h (angular width) are not well constrained and are fixed to be equal to 1 for B0 and 0.065 for h, on the basis of the literature [14]. However, we have compared the results obtained by the inversion in both cases (free and fixed opposition function) and verified that it has no impact upon the determination of the other Hapke parameters.

Differently from the opposition function parameters, b , c, $\bar{\theta}$, *w* are well constrained and their distribution wi-

thin the ROI can be mapped. In addition, a critical assessment analyis is carried out which establishes that for 95% of the pixel population the accuracy on the parameter determination is as follows : ±0.0075 for b and c, ± 0.9° for □, ± 0.005 for *w*. We also determine the degree of correlation between these 4 parameters (see table 1).

correlation	b	c	□	*w*
b	1	-0.95	0.74	0.79
c		1	-0.84	-0.78
□			1	0.67
w				1

Table 1. Intercorrelation coefficients between the photometric parameters.

Based on a Principal Component Analysis (PCA), a supervised classification is then derived from the examination of the photometric properties at the pixel scale. Six classes which reveal different photometric behaviors are identified and displayed on figure 2a and the corresponding distribution is shown on figure 2b. The yellow and red classes correspond respectively to the areas located in the mare regolith and « red halo » units as depicted earlier [9, 11]; despite the rather high *w* value ranging between 0.44 and 0.51, the photometric quantities are consistent with those in the literature [14, 15], with □ comprised between 19 and 25°, in agreement with mare regolith in situ determinations [7]. The photometric effect associated with the halo transpars mainly in the phase function parameters b and c. The light blue and pink (extreme photometric behavior) classes correspond to the bright part of the Reiner Gamma Formation (RGS unit in [9]); b and c values reveal a prevailing forward scattering behavior indicating a marked anisotropic response of the particulate medium constitutive of the local regolith ; the □ value ranges between 26 and 38°, suggesting the occurrence of a very pronounced mesoscale roughness at the submillimetric-centimetric scale [12], consistent with the presence of a very disturbed surface state with respect to the case of a standard mare regolith. The green class photometric characteristics appear intermediate between those of the yellow and light blue classes, suggesting spatial mixings. It corresponds to the dark furrow present within RGF in the ROI. Last but not the least, we also not the occurrence of pixels with no spatial connectivity coded in dark blue for which the □ roughness values are low, in the range of 19 to 23°, suggesting unusually smooth surface textures in agreement with [6,9].

Conclusions: The local variations of the RGF surface state which are mapped here support the hypothesis that the observed surface optical modifications analyzed by photometric modeling may result from the plowing of the regolith by a swarm of cometary fragments with local disruption of the regolith structure and fine fraction local redeposition [6, 9, 16]. These findings highlight the potential, for the characterisation of planetary regolith surfaces, of the upcoming in situ and orbital photometric observations to be acquired for Mars and the moon.

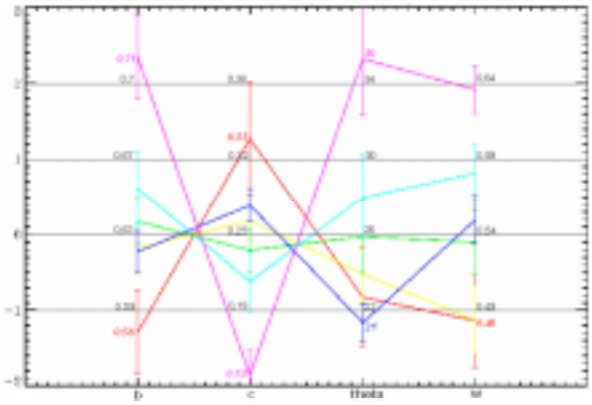

Figure 2a. Each color indicates one photometric class. Parameters b, c, ,□ and *w* are plotted from left to right with their mean and standard deviation.

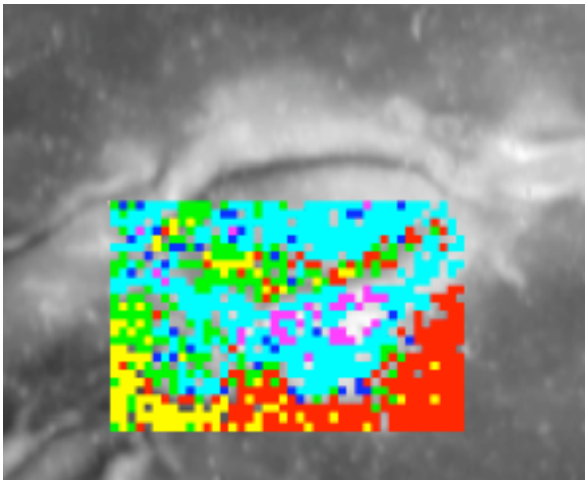

Figure 2b. Supervised classification associated with the 6 photometric classes mentioned above.

References : [1] Buratti et al., 1990, Icarus 84, 203. [2] Helfenstein et al., 1994, Icarus 107, 37 [3] De Grenier and Pinet, 1995, Icarus 115, 354 [4] Simonelli et al., 2000, Icarus 147, 353 [5] Clark et al., 2002, Icarus 155, 189 [6] Kreslavsky et al., 2000, J.Geophys. Res., 105, 20,281 ; Kreslavsky and Shkuratov, 2003, 108 [7] Helfenstein and Shepard, 1999, Icarus 141, 10 [8] Dollfus, 1998, Icarus 136, 69 [9] Pinet et al., 2000, J.Geophys. Res., 105, E4, 9457 [10] Shevchenko et al., 1993, Sol. Sys. Res 27, 310 [11] Schultz and Snrka, 1980, Nature 284, 22 ; Bell and Hawke, 1981, Proc. L.P.Conf. 12th, 679 [12] Cord et al., 2003, Icarus 165, 414 [13] Hillier and Buratti, 2001, Icarus 149, 251 [14] Hillier et al., 1999, Icarus 141, 205 [15] Helfenstein et al., 1997, Icarus 128, 2 [16] Starukhina and Shkuratov, 2003, Icarus, in press.